Open
ORIGINAL ARTICLE

Cell Research (2013) 23:491-507.

www.nature.com/cr

XBP-1u suppresses autophagy by promoting the degradation of FoxO1 in cancer cells

Ying Zhao[1], Xue Li[1], Mu-Yan Cai[2], Ke Ma[1], Jing Yang[1], Jingyi Zhou[1], Wan Fu[1], Fu-Zheng Wei[1], Lina Wang[1], Dan Xie[2], Wei-Guo Zhu[1, 3]

[1]Key Laboratory of Carcinogenesis and Translational Research of Ministry of Education, Department of Biochemistry and Molecular Biology, Peking University Health Science Center, Beijing 100191, China; [2]State Key Laboratory of Oncology in South China, Sun Yat-Sen University Cancer Center, Guangzhou, Guangdong 510060, China; [3]Peking-Tsinghua University Center for Life Sciences, Peking University, Beijing 100871, China

Autophagy is activated to maintain cellular energy homeostasis in response to nutrient starvation. However, autophagy is not persistently activated, which is poorly understood at a mechanistic level. Here, we report that turnover of FoxO1 is involved in the dynamic autophagic process caused by glutamine starvation. X-box-binding protein-1u (XBP-1u) has a critical role in FoxO1 degradation by recruiting FoxO1 to the 20S proteasome. In addition, the phosphorylation of XBP-1u by extracellular regulated protein kinases1/2 (ERK1/2) on Ser61 and Ser176 was found to be critical for the increased interaction between XBP-1u and FoxO1 upon glutamine starvation. Furthermore, knockdown of XBP-1u caused the sustained level of FoxO1 and the persistent activation of autophagy, leading to a significant decrease in cell viability. Finally, the inverse correlation between XBP-1u and FoxO1 expression agrees well with the expression profiles observed in many human cancer tissues. Thus, our findings link the dynamic process of autophagy to XBP-1u-induced FoxO1 degradation.

***Keywords*:** FoxO1; XBP-1u; ERK; autophagy; cancer
Cell Research (2013) **23**:491-507. doi:10.1038/cr.2013.2; published online 1 January 2013

Introduction

Autophagy is a process of intracellular degradation that delivers cytoplasmic constituents to the lysosome for the maintenance of homeostasis and bioenergetics in mammalian cells [1-4]. Autophagy is activated under a number of stressful conditions, including serum starvation and oxidative stress, as well as several conditions that lead to increased protein misfolding [1, 5]. Through the induction of autophagy, mammalian cells are able to obtain an influx of free amino acids and other essential nutrients. However, autophagy is rarely persistently activated in response to stress, but is instead activated in a dynamic manner to avoid autophagy-induced cell death. For example, autophagy commonly occurs during the first few hours of serum starvation, when it provides an initial burst of free amino acids for the synthesis of essential proteins; however, this autophagic process is rarely observed after the first 4-8 h of serum starvation in normal rat kidney cells or mouse fibroblasts [6, 7].

Several regulators have been reported to be important for the induction of autophagy, including beclin1, mammalian target of rapamycin (mTOR) and the FoxO family members [8-12]. Mammalian FoxO transcription factors, including FoxO1, FoxO3a, FoxO4 and FoxO6, are homologs of *Caenorhabditis elegans* abnormal dauer formation-16 (DAF-16) and *Drosophila* dFoxO [13-16]. FoxO transcription factors are involved in several important biological processes, such as cell cycle arrest, DNA repair, apoptosis, glucose metabolism and aging [13, 17]. Recent reports have also raised the possibility that FoxO family members are involved in the induction of autophagy via both transcription-dependent and -independent pathways [10-12, 18]. Loss of FoxO protein is also responsible for the attenuation of autophagy in

Correspondence: Wei-Guo Zhu[a], Ying Zhao[b]
Tel: +86-10-82802235
[a]E-mail: zhuweiguo@bjmu.edu.cn
[b]E-mail: zhaoying0812@ bjmu.edu.cn
Received 14 November 2012; revised 21 November 2012; accepted 22 November 2012; published online 1 January 2013

Drosophila, mouse muscle cells and several cancer cell lines [10-12, 19].

As FoxO family proteins are key regulators of multiple important biological processes, factors that influence the fate of FoxO1 are of great interest to researchers. It has been reported that the FoxO proteins are degraded via the proteasomal pathway in response to insulin and growth factors. Additionally, the oncoprotein S-phase kinase-associated protein 2 (Skp2) has been shown to ubiquitinate FoxO1 and promote its degradation [20]. FoxO1 is also degraded by the ubiquitin-proteasome pathway in Fao hepatoma cells, a process mediated by COP1 — a RING-finger E3 ubiquitin ligase [21]. Finally, the ubiquitin E3 ligase MDM2 can bind to FoxO1 or FoxO3 to promote the polyubiquitination and degradation of these proteins [22, 23]. In addition to the factors mentioned above, X-box-binding protein-1s (XBP-1s) has recently been reported to interact with FoxO1 and cause the ubiquitin-dependent proteasomal degradation of FoxO1 in MEF cells [24], although the mechanism of FoxO1 degradation induced by XBP-1s is not fully understood.

XBP-1s is a transcriptional activator of the unfolded protein response (UPR) and is also a critical factor for the regulation of genes involved in cell survival [25, 26]. Unconventional splicing of the XBP-1 mRNA can result in two alternate proteins, XBP-1s (the spliced form) and XBP-1u (the unspliced form). Following endoplasmic reticulum (ER) stress, the XBP-1 pre-mRNA is cleaved by the activated inositol-requiring enzyme 1 (IRE1) to form the "mature" (i.e., spliced) XBP-1 mRNA, which encodes XBP-1s [27]; XBP-1s can then bind to ER stress-response elements to induce the transcription of ER chaperones [28]. In addition to regulating the UPR, XBP-1 has also been implicated in the regulation of autophagy in the murine nervous system [29]. XBP-1 deficiency resulted in increased levels of FoxO1 and enhanced macroautophagy in cellular and animal models of Huntington's disease, although the authors did not interpret how XBP-1 deficiency is related to autophagy, and how FoxO1 level is negatively correlated with XBP-1 level [30].

In this study, our results demonstrate that FoxO1 turnover is highly associated with the dynamic autophagy process. Phosphorylation of XBP-1u by ERK is required for XBP-1u binding to FoxO1, which leads to localization of FoxO1 to the 20S proteasome for degradation. Interestingly, we also identified an inverse correlation between XBP-1u and FoxO1 expression in 229 cases of human colorectal cancer tissues. The relationship between XBP-1u and FoxO1 expression was also found to be highly correlated with p62 status in these cancer tissues, which suggests that XBP-1 is a critical protein for the promotion of tumor development.

Results

Dynamic induction of autophagy is associated with changes in FoxO1 levels

Starvation caused by the removal of all amino acids or treatment with Earle's balanced salt solution (EBSS) induces very rapid autophagy [31], which makes it difficult to study the dynamics of this process. To induce a long-term autophagic model, we used glutamine-free medium to starve human cancer cells. As shown in Figure 1A, autophagy was induced in the human colon cancer HCT116 cell line in response to glutamine starvation, which reached a peak at 24 h, as measured by p62 degradation and LC3-II accumulation, two common autophagic hallmarks. Interestingly, p62 degradation and LC3-II accumulation gradually returned to normal levels by 36 h post treatment (statistical data shown in Supplementary information, Figure S8). Autophagy was also directly observed by electron microscopy, which was used to monitor the formation of autophagosomes, as well as by fluorescent microscopy, which was used to observe LC-3-immunopositive punctate signals. Numerous vesicular structures with double membranes were commonly observed when HCT116 cells were incubated in glutamine-free medium for 12-24 h, but not after 48 h (Figure 1B). Under the same treatment conditions, punctate LC3 signals were consistently observed in the HCT116 cells. This staining significantly decreased by 36 h after glutamine starvation (Figure 1C and 1D), indicating that the observed autophagy was a dynamic process. Therefore, we sought to determine the key regulators controlling these changes. As FoxO1 acetylation is involved in regulating the autophagic process [10], we first measured FoxO1 levels in the treated cells. As shown in Figure 1A (lower panels), FoxO1 levels gradually decreased in response to glutamine starvation. Surprisingly, we found that FoxO1 acetylation increased by 2 h after glutamine starvation and reached a peak at 24 h after treatment, as detected with a co-immunoprecipitation assay (Figure 1A, lower panels, and 1D). FoxO1 acetylation was highly correlated with its interaction with Atg7 (Figure 1A, lower panels) and the autophagic changes induced by glutamine starvation in the HCT116 cells (Figure 1D). To measure the overall rates of long-lived protein degradation, HCT116 cells were pre-labeled with [^{3}H]-leucine 48 h prior to glutamine starvation in the presence or absence of 3-methyladenine (3-MA), an inhibitor of autophagy. Figure 1E shows that glutamine starvation significantly enhanced the overall degradation of proteins in HCT116 cells in a time-dependent manner. However,

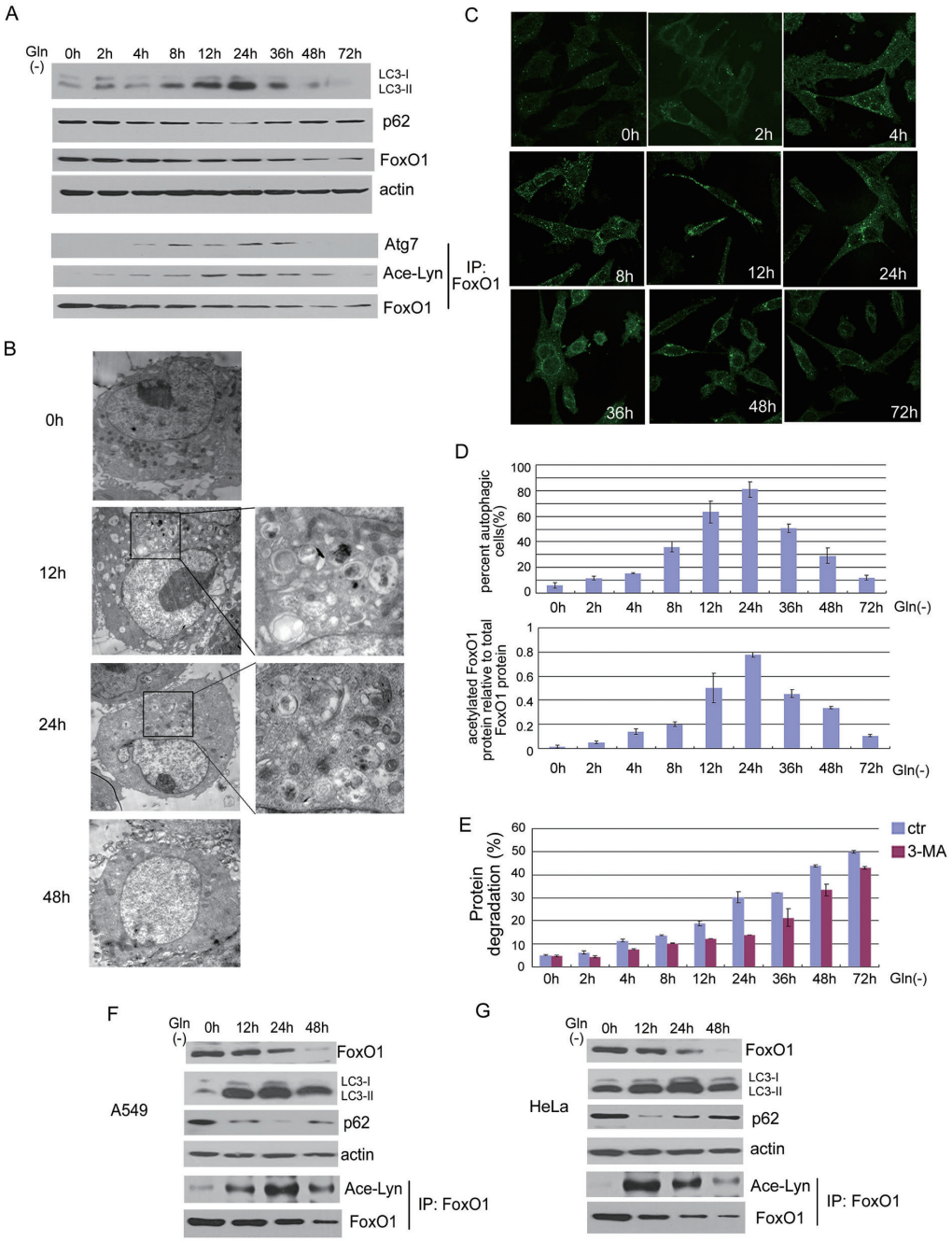

Figure 1 Dynamic induction of autophagy is associated with changes in FoxO1 levels. **(A)** Western blotting was performed to determine the levels of total FoxO1 expression, p62 degradation and LC3-II accumulation in HCT116 cells in response to glutamine starvation over 72 h (upper panels). Proteins were also extracted for co-immunoprecipitation with an anti-FoxO1 antibody and were probed with anti-Atg7 or anti-acetylated lysine (lower panels). **(B)** Electron micrographs showing autophagic vesicles in HCT116 cells that had been starved for up to 48 h. **(C)** LC3-immunopositive punctate signals were observed in HCT116 cells after glutamine starvation for up to 72 h. **(D)** A quantitative analysis of the LC3-positive punctate cells shown in **C** (upper panels). The criterion for being counted is cell with more than 10 puncta. An analysis of the changes in acetylated FoxO1 shown in **A** (lower panels). Each band was scanned and relative intensive average density was determined. The data are presented as the mean ± SD (n = 3). **(E)** HCT116 cells were labeled with [^{3}H]-leucine for 48 h, washed, incubated for 24 h and then subjected to glutamine starvation for up to 72 h in the presence or absence of 3-MA. The relative degradation of the long-lived proteins was measured by counting radioactivity. Data are mean ± SD (n = 3). **(F**, **G)** Western blotting was also performed to determine the levels of total FoxO1 expression, FoxO1 acetylation, p62 degradation and LC3-II accumulation in A549 **(F)**, or HeLa cells **(G)** in response to glutamine starvation over 48 h.

the 3-MA-sensitive degradation gradually decreased by 36 h after glutamine removal in HCT116 cells, indicating that the long-lived protein degradation by 36 h after glutamine starvation maybe depend on other forms of autophagy but not on macroautophagy [6].

To determine whether this phenomenon occurs in other cell lines, we also assayed FoxO1 protein levels and acetylation status in A549 and HeLa cell lines under glutamine-starvation conditions (FoxO1 was highly expressed in A549 and HeLa cells, but virtually no expression was detected in H1299 cells [10]). Similar to what we observed in the HCT116 cells, FoxO1 levels gradually decreased whereas FoxO1 acetylation increased following treatment, which were correlated with changes in p62 degradation and LC3-II accumulation in both cell lines (Figure 1F and 1G). These data suggest that the dynamic autophagic process is likely to be associated with FoxO1 acetylation.

FoxO1 is degraded by the 20S proteasome

To determine whether the reduction in FoxO1 protein levels was the result of protein degradation or gene repression, we measured FoxO1 mRNA levels using real-time PCR. Glutamine starvation had no effect on FoxO1 mRNA levels (Figure 2A), indicating that protein degradation was likely responsible for the decrease in FoxO1 protein levels after glutamine starvation.

To determine the pathways involved in FoxO1 degradation, we pretreated HCT116 cells with a panel of inhibitors, the proteasome inhibitor MG132, the calpain inhibitor calpeptin and the lysosome inhibitor chloroquine (CHQ). MG132 significantly blocked the glutamine starvation-induced reduction of FoxO1 levels (Figure 2B) whereas calpeptin and CHQ had no effect on FoxO1 degradation (Figure 2C). These results suggest that FoxO1 is degraded by the proteasomal pathway in response to glutamine starvation.

Next, to determine whether FoxO1 is degraded in the nucleus or the cytoplasm, we ectopically expressed FoxO1 in H1299 cells, a cell line that normally has very low levels of FoxO1 [10]. We generated plasmids to express flag-tagged wild-type FoxO1 (WT) or mutated FoxO1 (3A) in which the residues T24, S256 and S319 of FoxO1 were each changed to alanine. The mutant protein FoxO1 (3A) was predominantly localized to the nucleus. As shown in Figure 2D, a significant decrease in FoxO1 (WT) protein levels was observed in response to glutamine starvation, whereas FoxO1 (3A) protein levels were unchanged. To further characterize this process, nuclear and cytoplasmic fractions were prepared from glutamine-starved HCT116 cells and then subjected to immunoblotting with a FoxO1 antibody. As shown in Figure 2E, degradation of endogenous FoxO1 was only observed in the cytoplasmic fraction. Taken together, these data demonstrate that glutamine starvation-induced FoxO1 degradation occurs in the cytoplasm and not in the nucleus.

Finally, to determine whether ubiquitination is required for FoxO1 degradation, plasmids expressing flag-tagged FoxO1 or a HA-ubiquitin were co-transfected into H1299 cells; FoxO1 ubiquitination was detected by co-immunoprecipitation with an anti-flag antibody followed by immunoblotting with an anti-HA antibody. Contrary to our expectations, we were unable to detect any polyubiquitinated FoxO1 in H1299 cells in response to glutamine starvation (Figure 2F). Therefore, we investigated whether the 20S proteasome plays a role in FoxO1 degradation. As assayed by co-immunoprecipitation, flag-tagged FoxO1 was physically associated with the 20S proteasome (Figure 2G), which was further confirmed by an *in vitro* protein degradation assay (Figure 2H). These data suggest that FoxO1 is degraded by 20S proteasome.

XBP-1u is required for the glutamine starvation-induced FoxO1 degradation

Several possible molecules have been reported to be involved in the degradation of FoxO proteins, including Skp2 [20], MDM2 [22] or XBP-1s [24]. To determine whether these proteins are associated with FoxO1 degradation in response to glutamine starvation, we designed several siRNA fragments against these proteins. Using RNAi technique, we excluded Skp2 and MDM2 as the molecules required for FoxO1 degradation in response to glutamine starvation (data not shown). We next tested the role of XBP-1 in FoxO1 degradation by transfecting plasmids encoding XBP-1u or XBP-1s into HCT116 cells. XBP-1s is a nucleus-localized protein and XBP-1u is predominately localized in the cytoplasm (Supplementary information, Figure S1A). As shown in Figure 3A, the FoxO1 protein level was markedly reduced by overexpression of XBP-1u, but not by overexpression of XBP-1s. In addition, knockdown of XBP-1u significantly abrogated glutamine starvation-induced reduction of FoxO1 protein in HCT116 cells (Figure 3B and Supplementary information, Figure S1B). We also performed a rescue experiment using a plasmid specifically expressing mutated XBP-1u to validate the XBP-1u's activity in the induction of FoxO1 degradation in HCT116 cells. The XBP-1u expressing plasmid rescued the reduction of FoxO1 degradation by XBP-1u RNAi in the absence of glutamine (Figure 3C), further showing that XBP-1u is responsible for the cytosolic FoxO1 degradation in response to glutamine starvation.

To confirm the role of XBP-1u in the degradation of

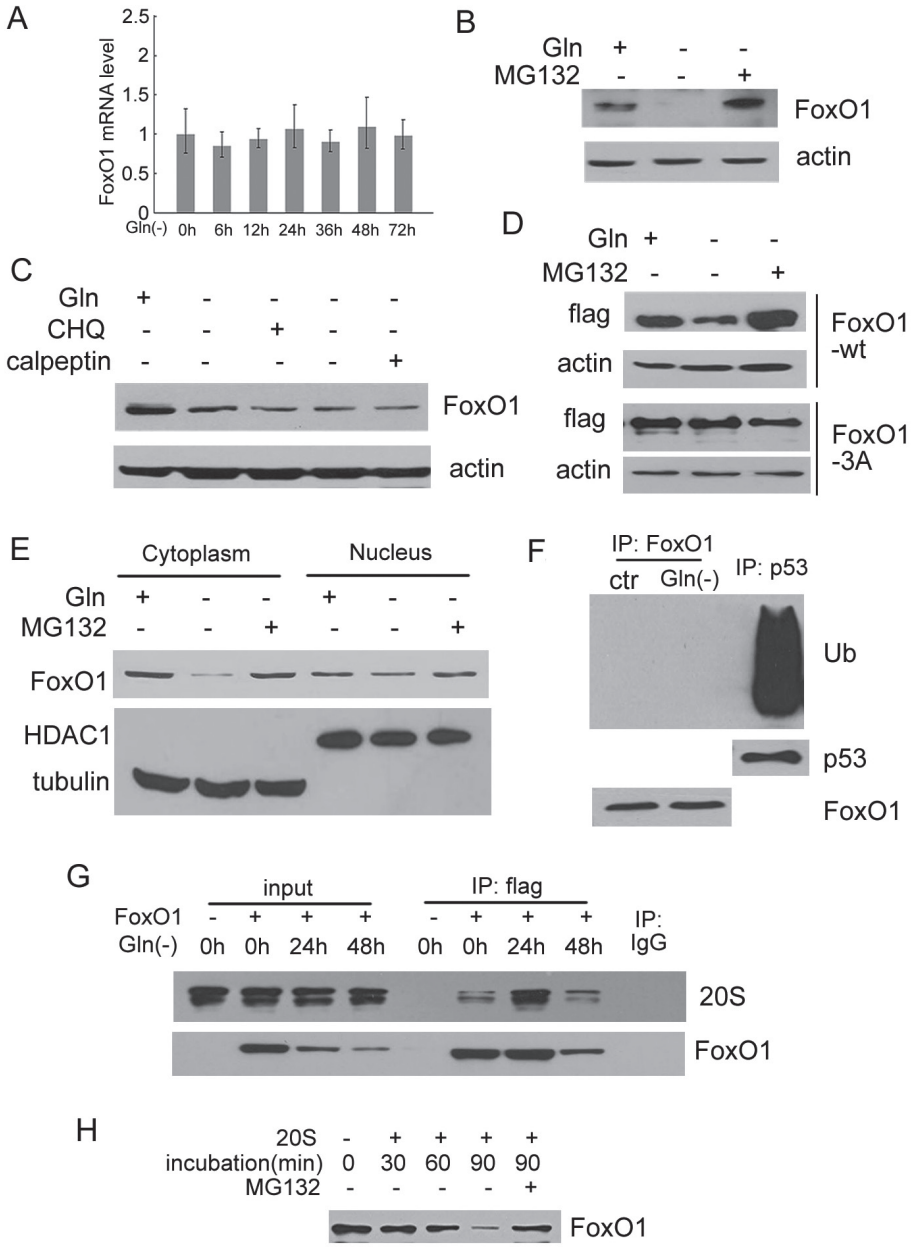

Figure 2 FoxO1 is degraded through the 20S proteasome pathway. **(A)** Quantitative PCR (qPCR) was performed to measure FoxO1 mRNA expression levels in HCT116 cells in response to glutamine starvation over 72 h. **(B**, **C)** Western blotting was performed to determine FoxO1 levels in HCT116 cells in response to glutamine starvation over 48 h with or without MG132 (2 μM) **(B)**, CHQ (10 μM) or calpeptin (50 μM) **(C)**. **(D)** H1299 cells were transfected with plasmids encoding FoxO1 (WT) or FoxO1 (3A). 24 h after transfection, H1299 cells were glutamine starved for 24 h in the presence or absence of MG132, proteins were then extracted, and western blotting was performed to detect changes in FoxO1 levels. **(E)** HCT116 cells were incubated in glutamine-free medium in the presence or absence of MG132 for 48 h. Nuclear and cytoplasmic proteins were extracted, and FoxO1 levels were analyzed by western blotting. HDAC1 was used as a loading control for nuclear proteins, and tubulin was used as a loading control for cytoplasmic proteins. **(F)** H1299 cells were cotransfected with plasmids encoding flag-FoxO1 and HA-ubiquitin, followed by incubation in glutamine-free medium in the presence of MG132 (2 μM) for 24 h. Cell lysates were immunoprecipitated with an anti-flag antibody and blotted with an anti-ubiquitin antibody. The bottom panel indicates equal amounts of FoxO1. Ubiquitination of p53 was used as a positive control. **(G)** H1299 cells were transfected with flag-FoxO1. 24 h after transfection, H1299 cells were glutamine starved for up to 48 h, and the cell lysates were immunoprecipitated with an anti-flag antibody and blotted with an anti-20S proteasome antibody. **(H)** *In vitro*-translated FoxO1 protein was incubated with 20S proteasome in the presence or absence of MG132 (10 μM) for up to 90 min. Following incubation, samples were examined by western blotting analysis.

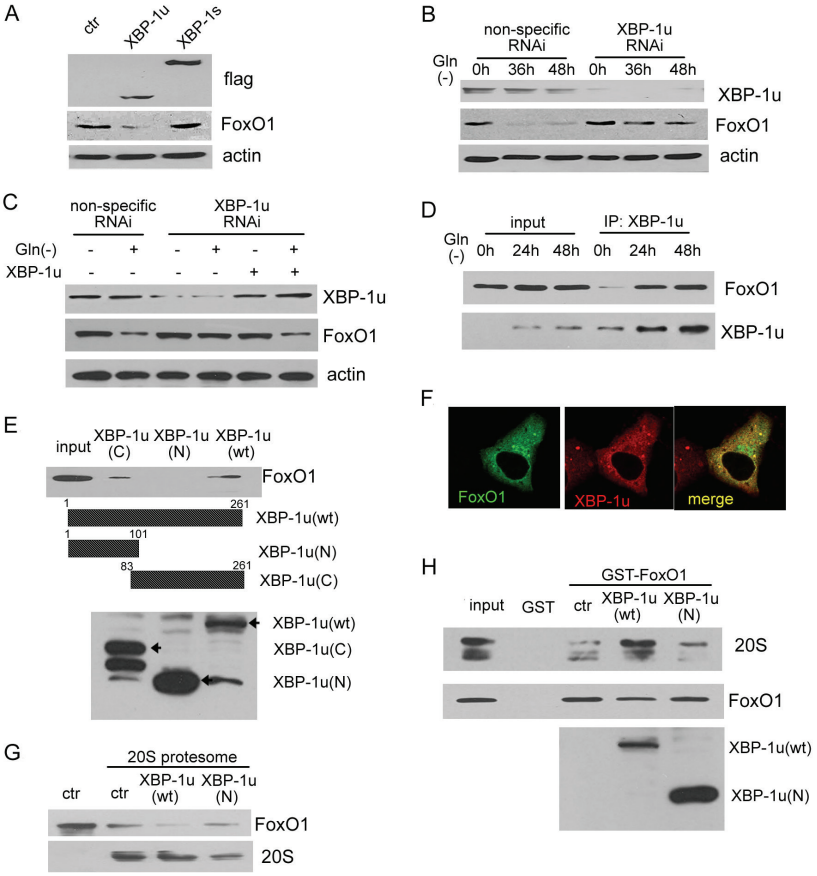

Figure 3 XBP-1u is involved in the induction of FoxO1 degradation. **(A)** Flag-tagged XBP-1u, XBP-1s or an empty plasmid were individually transfected into HCT116 cells, and endogenous FoxO1 protein levels were measured by western blotting. **(B)** HCT116 cells were transfected with XBP-1u-specific or non-specific siRNA. 48 h after transfection, HCT116 cells were glutamine starved for up to 48 h, and cell lysates were extracted for quantification of XBP-1u or FoxO1 levels. **(C)** A rescue experiment using a plasmid specifically expressing mutated XBP-1u was performed to validate XBP-1u's activity in the induction of FoxO1 degradation in HCT116 cells in the presence or absence of glutamine starvation. **(D)** HCT116 cells were glutamine starved for up to 48 h in the presense of MG132, and cell lysates were extracted for co-immunoprecipitation with an anti-XBP-1u antibody followed by probing with an anti-FoxO1 antibody. **(E)** Full-length XBP-1u as well as N- and C-terminal fragments of XBP-1u were expressed in bacteria and purified; these proteins were then incubated with *in vitro*-translated FoxO1. Western blotting was performed to detect the interaction of XBP-1u with FoxO1. **(F)** H1299 cells were co-transfected with plasmids encoding GFP-FoxO1 and flag-XBP-1u, and immunofluorescence was performed after staining with an anti-flag antibody. **(G)** *In vitro*-translated FoxO1 protein was incubated with 20S proteasome supplemented with GST (negative control) or various GST-XBP-1u fusion proteins; after 1 h incubation, the samples were examined by western blotting analysis. **(H)** GST or a GST-FoxO1 fusion protein was incubated with 20S proteasome in the presence or absence of *in vitro*-translated wild-type or mutant XBP-1u. The 20S proteasome and the GST-FoxO1 fusion protein were assayed by western blotting analysis.

FoxO1, we first tested whether XBP-1u interacts with FoxO1 using a co-immunoprecipitation assay. As shown in Figure 3D, endogenous FoxO1 interacted with XBP-1u in the presence of MG132 in the HCT116 cells after glutamine starvation. Next, to test whether the interaction between XBP-1u and FoxO1 was direct, an *in vitro* GST pull-down assay was carried out using bacterially expressed proteins. Wild-type FoxO1 protein that was translated *in vitro* was incubated with GST fusion proteins of full-length, C- or N-terminal XBP-1u; western blotting was then performed using an anti-FoxO1 antibody. As shown in Figure 3E, the C-terminal region of XBP-1u interacted with FoxO1. To examine the subcellular localization of the FoxO1 and XBP-1u interaction, we transfected H1299 cells with plasmids expressing GFP-FoxO1 and flag-XBP-1u, and performed immunofluorescence assays using an anti-flag antibody. We found that the majority of wild-type FoxO1 was present in the cytoplasm where it co-localized with XBP-1u in the absence or presence of glutamine (Figure 3F and Supple-

mentary information, Figure S1C). These results suggest that FoxO1 interacts with XBP-1u in the cytoplasm upon glutamine starvation.

Moreover, FoxO1 degradation by the 20S proteasome was enhanced by incubation with full-length XBP-1u protein. In contrast, N-terminal XBP-1u protein, which was not observed to directly interact with FoxO1, did not affect FoxO1 degradation by the 20S proteasome (Figure 3G and Supplementary information, Figure S2). Furthermore, we examined the effects of XBP-1u on the FoxO1/20S proteasome interaction. As shown in Figure 3H, the 20S proteasome fraction was able to interact with FoxO1 as demonstrated by a GST-FoxO1 pull-down assay. The addition of *in vitro* translated full-length XBP-1u, but not N-terminal XBP-1u, facilitated the FoxO1/20S proteasome interaction. Taken together, these data suggest that the interaction between XBP-1u and FoxO1 is required for degradation of FoxO1 by the 20S proteasome.

The ERK pathway is involved in XBP-1u-mediated FoxO1 degradation

Prior to degradation, FoxO1 is usually post-translationally modified by phosphorylation [32, 33]. Therefore, we used two well-characterized kinase inhibitors, PD098059, an inhibitor of ERK, and SB203580, an inhibitor of p38, to investigate which cellular signaling pathway might be involved in XBP-1u-mediated FoxO1 degradation. HCT116 cells were pre-incubated with PD098059 or SB203580 for 30 min followed by incubation with or without glutamine in the presence of inhibitor for further 24 h. Blockage of ERK by PD098059 completely inhibited glutamine starvation-induced FoxO1 degradation; SB203580 did not inhibit degradation (Figure 4A). To further confirm the role of ERK in FoxO1 degradation, HCT116 cells were transfected with non-specific or ERK-specific siRNA, and FoxO1 degradation was assayed. The efficiency of the RNAi against ERK was significant, and as expected, upon glutamine starvation, FoxO1 was degraded in the cells transfected with the control siRNA. In contrast, FoxO1 remained at a higher level in the cells transfected with the ERK siRNA (Figure 4B and Supplementary information, Figure 3A), suggesting that ERK plays a critical role in FoxO1 degradation.

To determine whether ERK directly phosphorylates FoxO1 to induce FoxO1 degradation, a plasmid encoding a mutated FoxO1 (9A) in which the nine putative ERK phosphorylation sites in FoxO1 were mutated to alanine, or a plasmid encoding wild-type FoxO1 (WT), were separately transfected into H1299 cells. Both FoxO1 (WT) and FoxO1 (9A) were degraded after glutamine starvation (Figure 4C), indicating that ERK-mediated FoxO1 degradation does not result from direct phosphorylation of FoxO1 by ERK.

As FoxO1 interacted with XBP-1u during glutamine starvation, we could not rule out the possibility that ERK might directly phosphorylate XBP-1u, and that in turn, phosphorylated XBP-1u might play a role in FoxO1 degradation. Indeed, we found that glutamine starvation induced phosphorylation of both endogenous and overexpressed XBP-1u in HCT116 cells, as shown by a co-immunoprecipitation assay (Figure 4D and Supplementary information, Figure S3B). Using the software program GPS2.1, we identified two residues in XBP-1u, Ser61 and Ser176, as putative ERK target sites. Therefore, we generated a plasmid encoding a mutated XBP-1u (S61/176A) in which the two serine residues were changed to alanine. After transfection into HCT116 cells, we confirmed that glutamine starvation did not induce XBP-1u (S61/176A) phosphorylation (Figure 4E and Supplementary information, Figure S3C). The purified XBP-1u and ERK1 were then incubated *in vitro* to investigate whether ERK is responsible for XBP-1u phosphorylation. As shown in Figure 4F, XBP-1u was significantly phosphorylated by ERK1. These data suggest that ERK activity may be required for XBP-1u to modulate degradation of FoxO1.

Phosphorylation of XBP-1u by ERK is critical for the increased interaction of XBP-1u and FoxO1

To test whether the phosphorylation of XBP-1u by ERK has any effect on the interaction of XBP-1u and FoxO1, HCT116 cells were treated with or without the ERK inhibitor PD098059 and then exposed to glutamine starvation. Figure 5A and Supplementary information, Figure S4A show that PD098059 significantly disrupted the interaction between FoxO1 and XBP-1u. To test whether the decreased interaction between FoxO1 and XBP-1u was due to changes in XBP-1u localization, we collected nuclear and cytoplasmic fractions from HCT116 cells that had been treated with or without PD098059 prior to glutamine starvation. Figures 5B, 5C and Supplementary information, Figure S4B show that the majority of cytoplasmic XBP-1u translocated into the nucleus in the presence of PD098059 during glutamine starvation. To further investigate the role of phosphorylation in the nuclear export of XBP-1u, the XBP-1u (WT), XBP-1u (S61A), XBP-1u (S176A) or XBP-1u (S61/176A) plasmids were separately transfected into H1299 cells, followed by immunostaining and/or nuclear/cytoplasmic extraction. As shown in Figures 5D, 5E and Supplementary information, Figure S4C, XBP-1u (S61/176A) was localized to both the nucleus

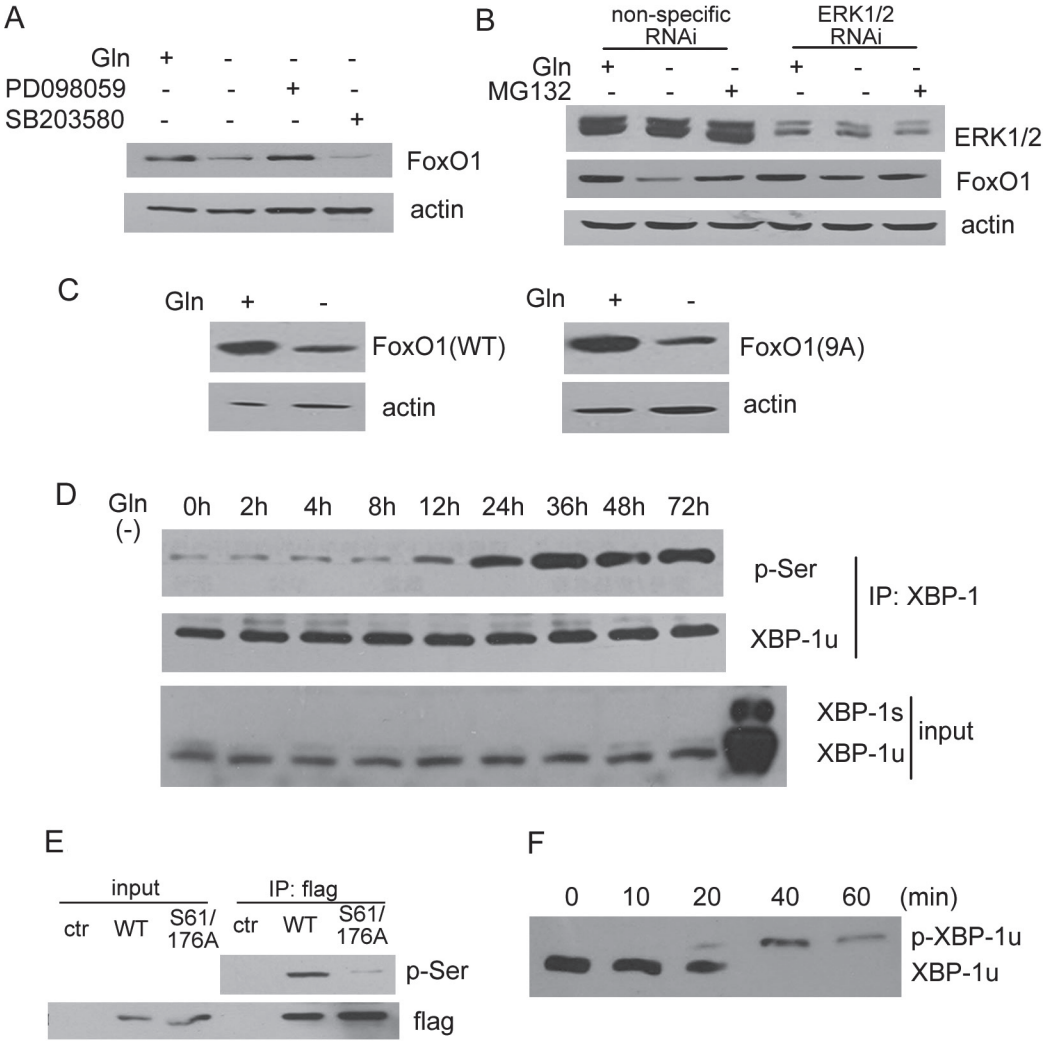

Figure 4 Activation of the ERK signaling pathway is involved in FoxO1 degradation. **(A)** Western blotting was performed to detect FoxO1 levels in HCT116 cells in the presence of PD098059 (10 μM) or SB203580 (10 μM) in response to glutamine starvation for 48 h. **(B)** HCT116 cells were transfected with ERK1/2-specific or non-specific siRNA. 48 h after transfection, HCT116 cells were glutamine starved for 24 h with or without MG132 (2 μM), and the cell lysates were then extracted for western blotting using anti-ERK1/2 or anti-FoxO1 antibodies. **(C)** H1299 cells were transfected with flag-tagged FoxO1 (WT) or FoxO1 (9A). 24 h after transfection, the cells were subjected to glutamine starvation for 24 h. The cell lysates were extracted and immunoblotted with anti-flag or anti-β-actin antibodies. **(D)** HCT116 cells were incubated in glutamine-free medium for up to 72 h, and cell lysates were extracted for co-immunoprecipitation with an anti-XBP-1u antibody and probed with anti-phosphoserine antibody. Cell extraction in which both XBP-1u and XBP-1s were overexpressed was used as a positive control. **(E)** HCT116 cells were transfected with plasmids encoding XBP-1u (WT) or XBP-1u (S61/176A). 24 h after transfection, the cell lysates were extracted for co-immunoprecipitation with an anti-XBP-1u antibody and probed with anti-phosphoserine antibody. **(F)** GST-XBP-1u was incubated with ERK1 at 30 °C for up to 60 min and the reaction was terminated by the addition of sample loading buffer. Then the mixtures were subjected to the Mn^{2+}-Phos-tag SDS-PAGE, and analyzed by western blotting using anti-XBP-1 antibody.

and the cytoplasm, whereas XBP-1u (WT) was mainly localized to the cytoplasm. The interaction of the 20S proteasome and XBP-1u was also disrupted when XBP-1u (S61/176A) was expressed in the presence or absence of glutamine (Figure 5F and Supplementary information, Figure S4E), indicating that Ser61 and Ser176 are essential for XBP-1u interaction with the 20S proteasome. Furthermore, XBP-1u mutants lacking ERK phosphorylation sites (S61/176A) or lacking 20S proteasome binding sites (1-204 aa) were also tested for their ability to

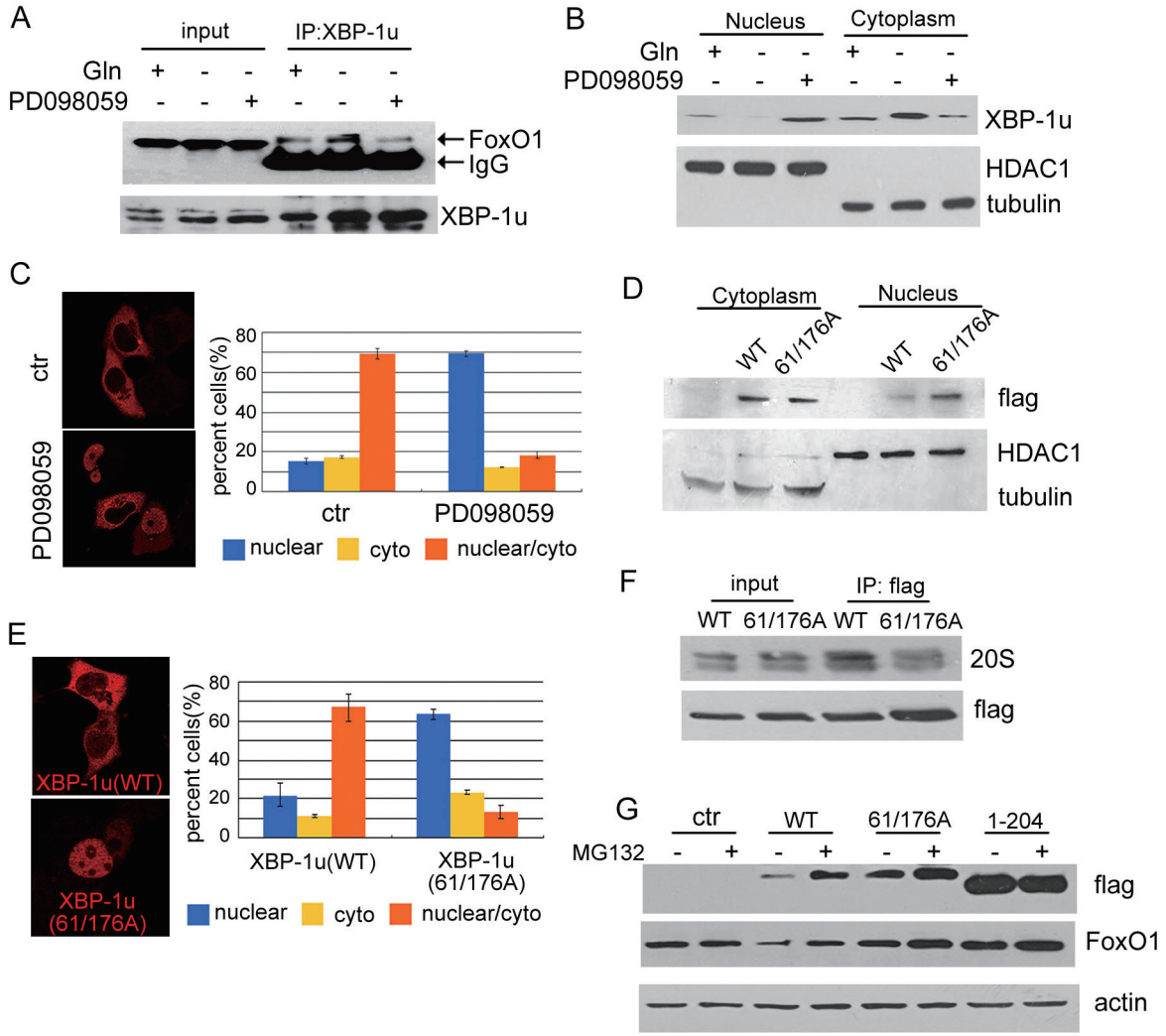

Figure 5 Phosphorylation of XBP-1u by ERK is critical for the increased interaction of XBP-1u and FoxO1. **(A)** HCT116 cells were incubated in glutamine-free medium in the presence or absence of PD098059 (10 μM) for 24 h. The cell lysates were extracted for co-immunoprecipitation with an anti-XBP-1u antibody and probed with an anti-FoxO1 antibody. **(B)** Cell fractions extracted from the above treatment were analyzed to determine the cellular localization of XBP-1u. HDAC1 was used as a loading control for nuclear proteins, and tubulin was used as a loading control for cytoplasmic protein. **(C)** Localization of XBP-1u was determined by transfection of a plasmid encoding flag-XBP-1u into HCT116 cells, which were incubated in glutamine-free medium in the presence or absence of PD098059. After 24 h of treatment, immunostaining was performed using an anti-flag antibody. For quantification, 100 cells per coverslip were counted, and the results are shown as the percentage of cells. The values shown in **C** are the mean ± SD (n = 3). **(D)** Nuclear and cytoplasmic proteins were extracted, and western blotting was performed to analyze the cellular localization of wild-type and mutant XBP-1u. **(E)** The localization of wild-type or mutant XBP-1u was determined by transfection of XBP-1u into HCT116 cells and immunostaining with an anti-flag antibody (left panel). For quantification, 100 cells per coverslip were counted, and the results are shown as the percentage of cells. The values shown in **E** are the mean ± SD (n = 3) (right panel). **(F)** 24 h after plasmids encoding flag-XBP-1u (WT) or flag-XBP-1u (S61/176A) were transfected into HCT116 cells, the cell lysates were extracted for co-immunoprecipitation with an anti-flag antibody and probed with an anti-20S proteasome antibody. **(G)** HCT116 cells were transfected with a control plasmid or plasmids encoding flag-XBP-1u (WT), flag-XBP-1u (S61/176A) or flag-XBP-1u (1-204) in the presence or absence of MG132 (2 μM). After 24 h of treatment, the cell lysates were extracted and immunoblotted with anti-flag, anti-FoxO1 or anti-β-actin antibodies.

destabilize FoxO1. Overexpression of XBP-1u (WT), but not the XBP-1u (S61/176A) or XBP-1u (1-204 aa) (Figure 5G), induced a decrease in FoxO1 protein levels. In addition, both single mutated XBP-1u (S61A) and

XBP-1u (S176A) also induced a modest degradation of FoxO1, but much less than WT XBP-1u (Supplementary information, Figure S4D). These data indicate that dephosphorylation of XBP-1u promotes XBP-1u translocation from the cytoplasm to the nucleus and attenuates its interaction with the 20S proteasome, which leads to a decrease in FoxO1 degradation.

Downregulation of XBP-1 enhances FoxO1-dependent autophagy

As FoxO1 is essential for the induction of autophagy in response to serum starvation or oxidative stress [10], we tested whether XBP-1u suppresses autophagy via induction of FoxO1 degradation. As shown in Figure 6A and Supplementary information, Figure S5A, overexpression of XBP-1u significantly decreased FoxO1 protein levels, and blocked the accumulation of LC3-II and degradation of p62 induced by glutamine starvation. Similarly, the number of LC3 puncta significantly decreased when glutamine-starved HCT116 cells were transfected with XBP-1u, but not with XBP-1s (Figure 6B). To further clarify the role that endogenous XBP-1u plays in the induction of autophagy, an XBP-1 RNAi plasmid was transfected into HCT116 cells to establish stable XBP-1-knockdown cell lines; a non-specific RNAi plasmid was used as a negative control. These cell lines were separately cultured in glutamine-free medium for up to 48 h. Cell lysates were extracted for western blotting to detect changes in p62 degradation and LC3-II accumulation. LC3-II levels dropped by 36 h after glutamine starvation in cells containing normal XBP-1 levels (Figure 1A), whereas in XBP-1-knockdown cells, LC3-II levels did not drop until 72 h after glutamine starvation (Figure 6C and Supplementary information, Figure S5B, statistical data shown in Supplementary information, Figure S8). Additionally, glutamine starvation-induced p62 degradation was markedly reduced in XBP-1-knockdown HCT116 cells compared with control cells (Figure 6C, statistical data shown in Supplementary information, Figure S8). Consistently, even at 48 h after glutamine starvation, the number of autophagic cells did not drop in the XBP-1-knockdown cell lines as observed by fluorescent or electron microscopy (Figure 6D and 6E). We also performed the long-lived protein degradation assay in XBP-1-knockdown HCT116 cells. The 3-MA-sensitive degradation was persistently increased after glutamine removal (Figure 6F). In contrast, in FoxO1/XBP-1 double knockdown HCT116 cells, glutamine starvation did not induce p62 degradation or LC3-II accumulation (Figure 6G). These data indicate that downregulation of XBP-1 promotes autophagy and that this function requires FoxO1.

Persistent activation of autophagy by XBP-1 knockdown is associated with cell death

It is well known that autophagic death is a non-apoptotic form of programmed cell death. To investigate whether autophagy induced by XBP-1 knockdown has an effect on the overall survival of cancer cells, we tested the viability of HCT116 cells with or without XBP-1 knockdown under conditions of glutamine starvation. As expected, following glutamine starvation for 72 h, cell viability was significantly decreased in XBP-1-knockdown HCT116 cells compared with wild-type HCT116 cells (Figure 7A). Interestingly, cell death was inhibited in HCT116 cell lines that were stably transfected with the XBP-

Figure 6 Downregulation of XBP-1u induces autophagy. **(A)** HCT116 cells were transfected with a control plasmid or a plasmid encoding flag-XBP-1u or flag-XBP-1s. 24 h after transfection, the cells were subjected to glutamine starvation for 12 h in the presence or absence of E64/pepstatin A. The cell lysates were extracted and immunoblotted with anti-flag, anti-FoxO1, anti-LC3, anti-p62 or anti-β-actin antibodies. **(B)** HCT116 cells were transfected with a control plasmid or a plasmid encoding flag-XBP-1u or flag-XBP-1s. 24 h after transfection, the cells were subjected to glutamine starvation for 24 h, and the formation of LC3 punctate signals was observed (left panels). The criterion for being counted is cell with more than 10 puncta. Quantification of the ratio of LC3 punctate cells to total HCT116 cells is shown in the right panel. Values shown in **B** are the mean ± SD (n = 3). **(C)** Stable XBP-1-RNAi HCT116 cells were incubated in glutamine-free medium for up to 72 h. The cell lysates were extracted and immunoblotted with anti-FoxO1, anti-LC3, anti-p62 or anti-β-actin antibodies. **(D)** Stable XBP-1-RNAi HCT116 cells were incubated in glutamine-free medium for 72 h and the formation of LC3 punctate signals was observed (upper panels). Quantification of the ratio of LC3 punctate cells to total HCT116 cells is shown in the lower panel. The criterion for being counted is cell with more than 10 puncta. Values in **D** are the mean ± SD (n = 3) (lower panel). **(E)** Electron micrographs showing autophagic vesicles in the stable XBP-1-RNAi HCT116 cell line incubated in glutamine-free medium over 48 h. **(F)** Stable HCT116 cell line with XBP-1-RNAi was labeled with [^{3}H]-leucine for 48 h, washed, incubated for 24 h and then subjected to glutamine starvation for up to 72 h in the presence or absence of 3-MA. The relative degradation of long-lived proteins was measured by counting radioactivity. Data are mean ± SD (n = 3). **(G)** HCT116 cells and HCT116 cell lines stably expressing XBP-1-RNAi or XBP-1/FoxO1 double RNAi were incubated in glutamine-free medium for 48 h in the presence or absence of E64/pepstatin A. The cell lysates were extracted and immunoblotted with anti-XBP-1u, anti-FoxO1, anti-LC3, anti-p62 or anti-β-actin antibodies.

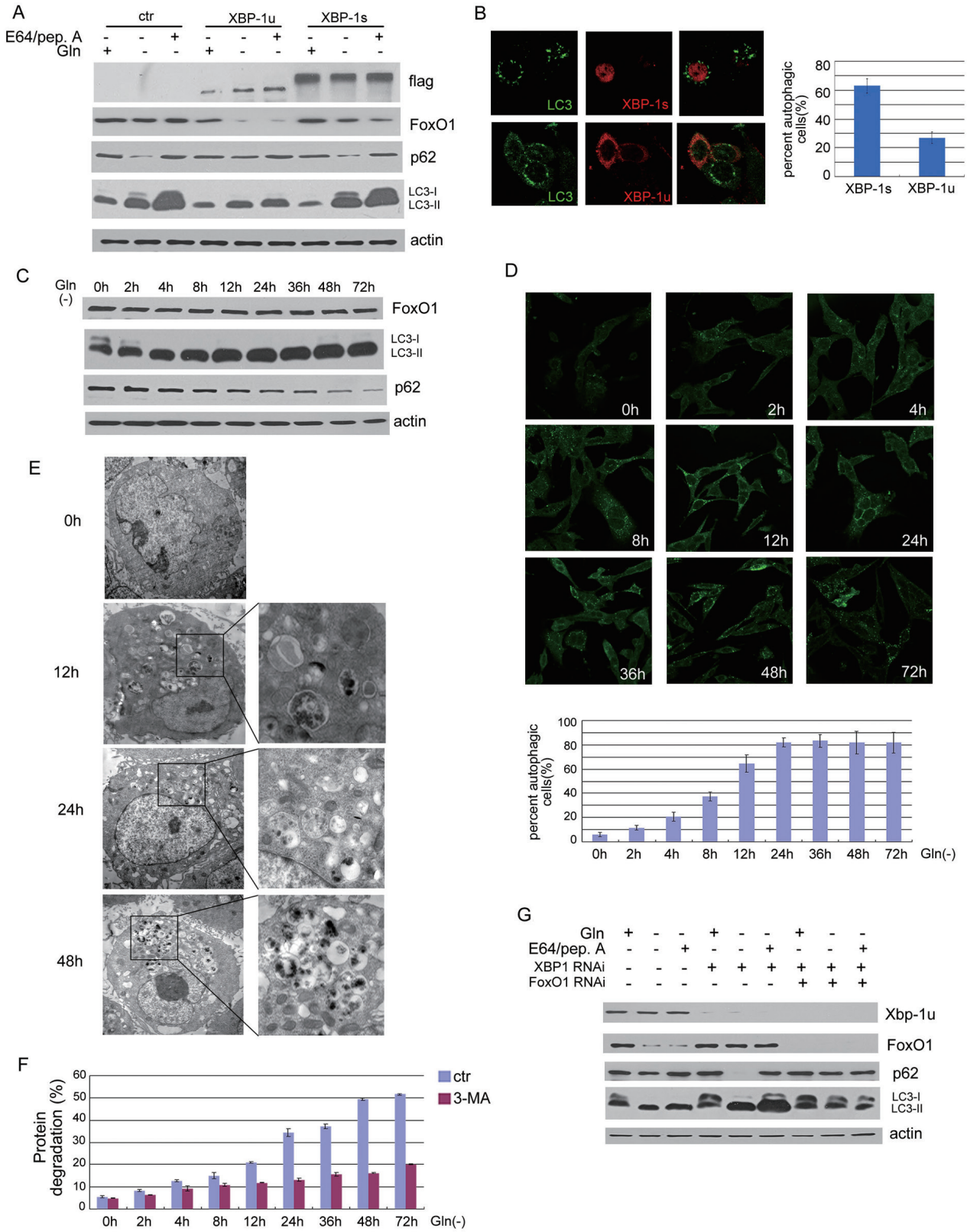
A
ctr
XBP-1u
XBP-1s
E64/pep. A
Gln
flag
FoxO1
p62
LC3-I
LC3-II
actin
B
LC3
XBP-1s
LC3
XBP-1u
percent autophagic cells(%)
XBP-1s
XBP-1u
C
Gln (-)
0h 2h 4h 8h 12h 24h 36h 48h 72h
FoxO1
LC3-I
LC3-II
p62
actin
D
0h
2h
4h
8h
12h
24h
36h
48h
72h
percent autophagic cells(%)
Gln(-)
E
0h
12h
24h
48h
F
Protein degradation (%)
ctr
3-MA
Gln(-)
G
Gln
E64/pep. A
XBP1 RNAi
FoxO1 RNAi
Xbp-1u
FoxO1
p62
LC3-I
LC3-II
actin

1- and FoxO1-RNAi plasmids, suggesting that XBP-1 knockdown-induced cell death upon glutamine starvation is dependent on FoxO1 (Figure 7A). To determine which type of cell death was occurring after XBP-1 knockdown, the autophagy inhibitor 3-MA or the apoptosis inhibitor Z-VAD-fmk were used. The cell death was greatly suppressed by 3-MA, verifying the role of autophagy in cell death caused by XBP-1 knockdown upon glutamine starvation (Figure 7B). These data suggest that persistent induction of autophagy induces cell death, which likely results from excessive degradation of cell components essential for survival.

Significant correlations between XBP-1u, FoxO1 and p62 expressions are demonstrated in human column rectum cancer (CRC) tissues

To investigate the expression profiles of XBP-1, FoxO1 and p62 in CRCs, we conducted immunohistochemical (IHC) staining for XBP-1u, FoxO1 and p62 on a CRC-TMA containing 229 CRC specimens. Using the criteria described in Materials and Methods, high expression of cytoplasmic XBP-1, FoxO1 and p62 was observed in 120 (52.4%), 107 (46.7%) and 119 (52.0%) of the 229 CRC cases, respectively. Representative IHC stainings of XBP-1u, FoxO1 and p62 are shown in Figure 7C and 7D. A correlation analysis demonstrates that the expression levels of XBP-1u in CRCs are inversely correlated with the expression levels of FoxO1 ($P < 0.05$) (Table 1). In addition, the expression profiles of XBP-1u and FoxO1 in this CRC cohort were positively and negatively correlated with p62 expression, respectively ($P < 0.05$) (Table 1). Importantly, we also found that high levels of XBP-1u or low levels of FoxO1 were significantly associated with the survival of CRC patients after surgery, as well as tumors in the lymph node and/or distant metastasis and a more advanced clinical stage (Supplementary information, Figure S7, Tables S1 and S2). These data further support the hypothesis that the correct balance of XBP-1u and FoxO1 activities is a critical factor that influences the development of cancer.

Discussion

In this study, we provide evidence that autophagy induced by glutamine starvation is a dynamic process that is highly associated with the turnover of FoxO1 protein. XBP-1u binds to FoxO1 and recruits FoxO1 to the 20S proteasome for degradation. This interaction between XBP-1u and FoxO1 is greatly enhanced by ERK1/2, which specifically catalyzes the phosphorylation of XBP-1u at Ser61 and Ser176; this suggests that cellular signaling pathways regulate the autophagic process by influencing FoxO1 levels (Figure 7E).

Earlier studies have shown that macroautophagy is a constitutively activated process [6, 7, 34, 35]. It was believed that macroautophagy was activated during the first hours of serum deprivation but then gradually returned to basal levels. If starvation continued beyond that time, the decrease in macroautophagy was concomitant with a progressive increase in chaperone-mediated autophagy (CMA), which benefitted cell survival [35]. In CMA-deficient cells, the high rates of sustained protein degradation in response to serum starvation were offset by upregulation of macroautophagy [34]. It is known that mTOR, an important autophagy repressor, is reactivated by the degradation of autolysosomal products in a dynamic manner [7]. Upon mTOR reactivation, tubules extend from autolysosomal membranes and give rise to vesicles that ultimately form functional lysosomes [7]. Consistent with previous reports, we also found that autophagy decreased after long-term glutamine starvation treatment (Figure 1), which suggests that even in cancer cells autophagy is a dynamic process. Furthermore, FoxO1 turnover may be an important factor used by cancer cells to control the autophagic process that occurs in response to glutamine starvation.

It has been reported that the degradation of FoxO family proteins is mediated by the ubiquitin-proteasome

Table 1 Correlations between expressions of XBP-1, FoxO1 and p62 in 229 colorectal carcinomas

		XBP-1 expression			FoxO1 expression		
	All cases	Low	High	*P* value*	Low	High	*P* value*
FoxO1 expression				0.016			
High	107	60 (56.1%)	47 (43.9%)				
Low	122	49 (40.2%)	73 (59.8%)				
p62 expression				0.005			0.005
Low	110	63 (57.3%)	47 (42.7%)		48 (43.6%)	62 (56.4%)	
High	119	46 (38.7%)	73 (61.3%)		74 (62.2%)	45 (37.8%)	

*Chi-square test.

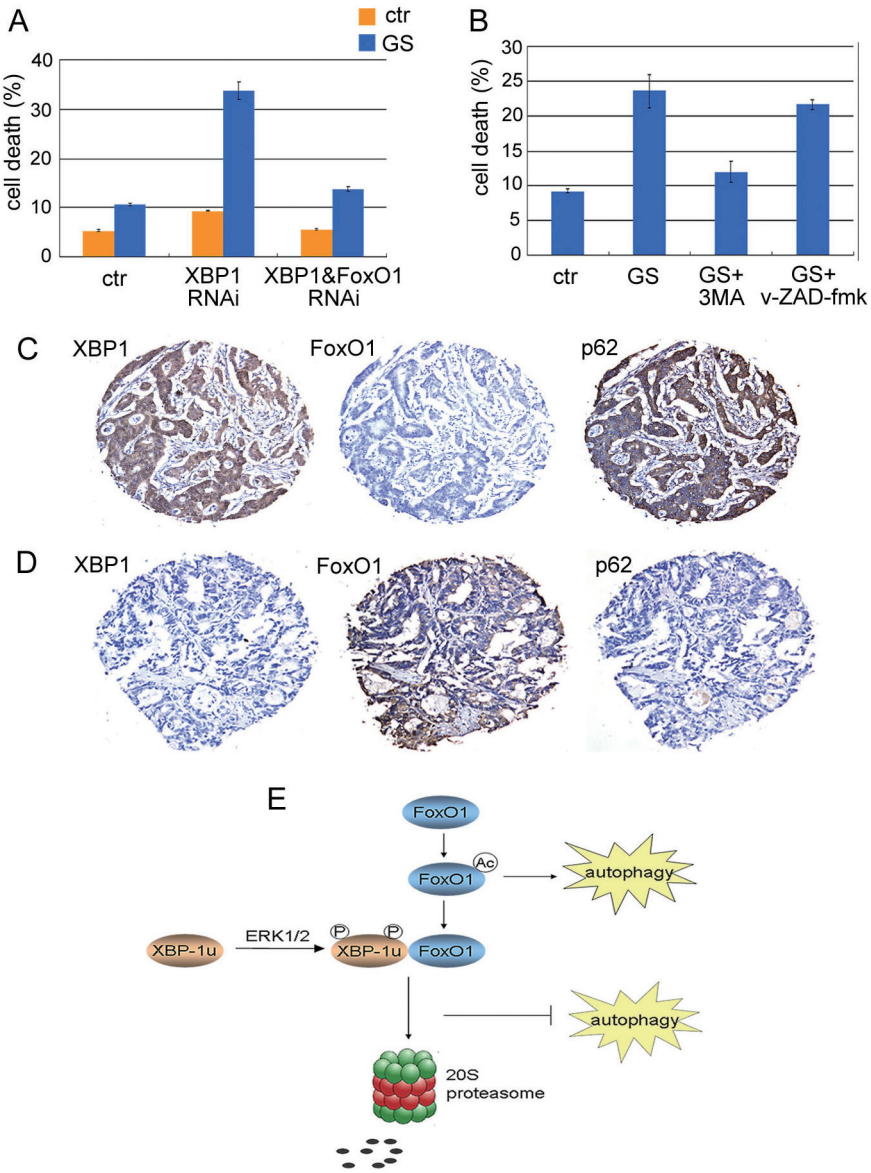

Figure 7 The expression levels of XBP-1u and FoxO1 are associated with cell viability and are inversely correlated in human cancer samples. **(A)** HCT116 cells and HCT116 cell lines stably expressing XBP-1 RNAi or XBP-1/FoxO1 double RNAi were glutamine starved, and cells were stained with PI 72 h after treatment. PI-stained (dead) cells were counted by flow cytometry and the percent of cell death was represented. Values are the mean ± SD (n = 3). **(B)** Stable XBP-1 RNAi HCT116 cell lines were glutamine starved for 72 h in the presence or absence of 3-MA (10 mM), or in the presence or absence of Z-VAD-fmk (50 μM). The number of cells was counted after staining with PI. Values are the mean ± SD (n = 3). **(C**, **D)** Immunohistochemical stainings of XBP-1, FoxO1 and p62 in CRC tissues. A CRC sample (case 26) showing high expression of XBP-1 and p62 and a low expression of FoxO1 in tumor cells **(C)**. Another CRC sample (case 139) showing high expression of FoxO1 and low expression of both XBP-1 and p62 in tumor cells **(D)**. **(E)** A schematic model showing the relationship between autophagy and XBP-1u-induced FoxO1 degradation in response to glutamine starvation.

pathway [32, 33, 36]. It has also been demonstrated that XBP-1s targets FoxO1 for ubiquitin-dependent degradation in MEF cells [24]. In this study, however, we demonstrate that XBP-1u is also a key regulator that modulates FoxO1 degradation in response to glutamine starvation. We believe that the conflicting results uncovered by our group and others on the specific isoform of XBP-1 that is involved in the degradation of FoxO1 could be explained by the different cell lines used in the respective studies; cancer cell lines were used in our study, and MEFs were

used in the other study. In addition, differences in treatment conditions might also cause cells to use alternative responses to induce FoxO1 degradation; for example, we exposed cells to glutamine-free medium, whereas the other group used normal medium. Nevertheless, we present several important pieces of evidence that XBP-1u is a true regulator of FoxO1 degradation. First, glutamine starvation induced a significant increase in XBP-1u mRNA levels but only slightly increased XBP-1s mRNA levels (Supplementary information, Figure S6). Second, it was found that FoxO1 degradation occurred only in the cytoplasm and that XBP-1u directly interacted with FoxO1 (Figures 2D, 2E, 3D and 3E); however, XBP-1s was found to be localized to nucleus, which would make it difficult to directly induce FoxO1 degradation in response to glutamine starvation. Third, we demonstrate that XBP-1u recruits FoxO1 into the 20S proteasome for ubiquitin-independent degradation (Figure 3G and 3H). Consistent with our data, XBP-1u has also been reported to play an important role in protein degradation in HeLa cells. XBP-1s (or ATF6) forms a complex with XBP-1u that is degraded by the proteasome; the degradation domain in the C-terminus of XBP-1u is critical for the interaction between XBP-1u and 20S proteasome [37, 38]. Consistent with other studies, we found that overexpression of wild-type XBP-1u, but not XBP-1u lacking proteasome binding sites (1-204 aa), was sufficient to decrease FoxO1 protein levels (Figure 5G).

It has been reported that ERK directly phosphorylates FoxO3 and that phosphorylated FoxO3 can be degraded via the MDM2-mediated ubiquitin-proteasome pathway [22]. However, in this study, the phosphorylation of FoxO1 may not be the key modification for ERK1/2-mediated FoxO1 degradation (Figure 4C). For example, although FoxO1 is degraded by the 20S proteasome *in vitro*, it is fairly stable *in vivo*, suggesting that the FoxO1 protein may not be easily accessible to the 20S proteasome in cells. Therefore, the modification of other FoxO1-interacting proteins, such as XBP-1u, is likely to contribute to FoxO1 destabilization in response to glutamine starvation. It is possible that upon glutamine starvation, XBP-1u undergoes phosphorylation-induced conformational changes to facilitate the entry of FoxO1 into the channel of the 20S proteasome.

XBP-1s can be phosphorylated by p38 MAPK on Thr48 and Ser61, which results in the nuclear translocation and increased stability of XBP-1s [39]. Our results show that ERK is also an important regulator of XBP-1u localization. After phosphorylation on Ser61 and Ser176, XBP-1u is prone to localize to the cytoplasm and interact with the 20S proteasome, leading to degradation of XBP-1u and FoxO1. Substitution of Ser61 and Ser176 in XBP-1u with alanine (Ser61/176A) diminishes the capacity of XBP-1u to drive FoxO1 degradation (Figure 5G). These data support the notion that ERK-dependent phosphorylation of XBP-1u on Ser61 and Ser176 plays a significant role in enabling the rapid destabilization and inactivation of FoxO1.

A growing body of evidence suggests that the autophagy can protect cells against cell death as well as mediate autophagic cell death [40-42]. In response to starvation, autophagy appears to be a cytoprotective process, as cells degrade non-essential components in order to generate the essential nutrients to meet the cell's energetic demands and maintain biosynthetic reactions [43, 44]. However, autophagy is also involved in cell death, which is caused by the progressive destruction of all cytoplasmic structures, including mitochondria [45, 46]. Our study suggests that autophagy is a protective mechanism under starvation conditions, as long as the autophagic process is not persistently activated. Once autophagy becomes constitutively activated, it induces cell death, which is most likely the result of excessive degradation of essential cellular components. Consistently, we found that after glutamine starvation the maintenance of FoxO1 activity by knocking down XBP-1u was sufficient to decrease cell viability in an autophagy-dependent manner (Figure 7A and 7B). Interestingly, a recent study also shows that XBP-1 deficiency in mice led to increased expression of FoxO1 that may be related to an enhanced autophagy in neurons [29], further supporting that XBP-1 level is negatively related to FoxO1 level and autophagy. Furthermore, the repression of XBP-1 expression has been shown to inhibit tumor development in animal models [47] and human tumor tissues [48]. Consistent with this, we also found that XBP-1u is highly expressed in human colon cancer samples, whereas FoxO1 is weakly expressed (Figure 7C and 7D). Taken together, our data suggest that the relationship between XBP-1u and FoxO1 may have significant relevance to clinical research.

In conclusion, turnover of FoxO1 may be an important mechanism that allows cells to modulate the autophagic process. In response to glutamine starvation, phosphorylated XBP-1u binds to FoxO1 and induces FoxO1 degradation. Therefore, targeting XBP-1u may be a useful strategy for the development of novel cancer therapies in the future.

Materials and Methods

Cell culture

A549, HCT116 and H1299 cells were grown in DMEM supplemented with 10% fetal bovine serum (heat inactivated at 56 °C for 45 min) and the appropriate amount of penicillin/streptomycin in a 37 °C incubator with a humidified, 5% CO_2 atmosphere.

Plasmids

Flag-XBP-1u and XBP-1u plasmids were kindly provided by Dr Ling Qi (Cornell University, USA). GST-XBP-1, GST-XBP-1 (1-101) and GST-XBP-1 (83-261) were kindly provided by Dr Qinong Ye (Beijing Institute of Biotechnology, China). FoxO1 (9A) was kindly provided by Dr Akiyoshi Fukamizu (University of Tsukuba, Japan).

Immunoblot analysis and immunoprecipitation assay

Protein expression was detected by western blotting as previously described with minor modifications. Equal amounts of proteins (100 to 150 μg) were separated by 9% to 15% SDS-PAGE. The antibodies used are anti-XBP-1 (Santa Cruz), anti-FoxO1 (#9462, Cell Signaling), anti-20S proteasome (Santa Cruz), anti-LC3 (Cell Signaling), anti-actin (Santa Cruz), anti-Flag (sigma), p62 (MBL) and anti-GFP (Santa Cruz).

For immunoprecipitation, cells were harvested and then lysed in NP-40 buffer supplemented with a complete protease inhibitor cocktail (Roche). Whole-cell lysates were used for immunoprecipitation with the indicated antibodies. Generally, 1-4 μg of commercial antibody was added to 1 ml of cell lysate, which was incubated at 4 °C for 8-12 h. After addition of protein A/G agarose beads, the incubation was continued for 1 h. Immunoprecipitates were extensively washed with lysis buffer and eluted with SDS loading buffer by boiling for 5 min.

RT-PCR

Primers for human XBP-1 were 5'-CCTGGTTGCTGAAGAGGAGG-3' (forward) and 5'-CCATGGGGAGATGTTCTGGAG-3' (reverse). Primers for human XBP-1u real-time PCR were 5'-ATGGATTCTGGCGGTATT-3' and 5'-AAGGGAGGCTGGTAAGG-3'.

Cellular fractionation

Cells were suspended in buffer A (10 mM Hepes, pH 7.9, 10 mM KCl, 0.1 mM EDTA, 0.1 mM EGTA, 1 mM DTT, 0.15% NP-40 and 1% cocktail), swollen for 10 min on ice, and centrifuged at 12 000× *g* for 30 s. Supernatant was collected as a cytoplasmic extract. The pellet was washed, resuspended in buffer B (20 mM Hepes, pH 7.9, 400 mM NaCl, 1 mM EDTA, 1 mM EGTA, 1 mM DTT, 0.5% NP-40 and 1% cocktail), and rocked for 15 min at 4 °C. The supernatant after centrifugation was used as nuclear extract.

Immunofluorescence analysis

Cells were cultured to ~80% confluency using the Chamber Slide System. After stress treatment, cells were fixed with 4% paraformaldehyde and permeabilized with methanol. Chamber slides were incubated with blocking solution (2% BSA in PBS), treated with primary antibody (1:100 dilution for all of the antibodies) overnight at 4 °C. After washed 3 times with blocking buffer, sides were treated with FITC/TRITC as the secondary antibody. Microscopic observation was performed using an Olympus BX-51 Research Microscope.

Purification of GST fusion proteins and GST pull-down experiments

GST or GST fusion proteins were expressed in *E. coli* BL21 (Tiangen Biotechnology, Beijing, China), induced with 0.1 mM isopropyl-1-thio-β-D-galactopyranoside for 12 h at 16 °C, and purified following the protocol from Amersham Biosciences. Equal amounts of GST or GST fusion proteins were incubated with glutathione-Sepharose 4B beads (Amersham Biosciences) by rocking at 4 °C for 1 h, and the beads were then washed three times with TEN buffer (20 mM Tris-HCl, pH 7.4, 0.1 mM EDTA and 100 mM NaCl). Total cell extracts from HCT116 cells were added to the beads and incubated by rocking at 4 °C overnight. The beads were washed three times with TENT buffer (0.5% NP-40, 20 mM Tris-HCl, pH 7.4, 0.1 mM EDTA and 300 mM NaCl), and then dissolved in 2× SDS loading buffer after centrifugation and boiled for 5 min at 100 °C. After centrifuging, the supernatant was extracted and analyzed by western blotting.

Long-lived protein degradation assay

Cells were grown in a 12-well plate (1 ml DMEM with 10% FBS per well) 1 day prior to the experiment. Cells were washed, incubated with leucine-free medium (leucine-free DMEM + 10% FBS) for 1 h to exclude endogenous leucine, and 5 Ci/ml [^{3}H]-leucine was added into the medium in the presence of 1 ml leucine-free DMEM with 10% dialyzed FBS for 48 h incubation. After washing three times with 1 ml of DMEM containing 2 mM unlabelled leucine, the cells were incubated in DMEM (containing 10% FBS and 2 mM unlabelled leucine) for 24 h to degrade short-lived proteins. After transfection and starvation, cell aliquots (100 μl) were taken to detect radioactivity (count per minute, cpm) at different time points. The medium was removed, and cells were lysed and placed into a vial to determine the total incorporated radioactivity. The protein degradation rate was calculated as cpm in the medium divided by the total incorporated cpm.

20S proteasome degradation assay

GST-FoxO1 and XBP-1u/XBP-1u^{NT} were incubated at 37 °C in HEPES buffer (50 mM HEPES, pH 7.5, 1 mM DTT and 0.018% SDS) in the presence of 20S proteasomes for 1 h. Samples from reaction mixtures were subjected to immunoblot analysis.

In vivo phosphorylation analysis of XBP-1u with phos-tag acrylamide gel electrophoresis

In the Mn^{2+}-Phos-tag-modified acrylamide gel, the phosphorylated proteins migrate slower than non-phosphorylated proteins by the interaction of phosphate groups with Mn^{2+}-Phos-tag (NARD Institute, Ltd., Hyogo, Japan). GST-XBP-1u was incubated alone or with GST-ERK (MERCK) in the kinase buffer (40 mM Tris-HCl, pH 7.5, 80 mM NaCl, 8 mM $MgCl_2$, 0.8 mM DDT and 50 μM ATP) in a total volume of 50 μl. Reaction mixtures were incubated at 30 °C for up to 60 min and were terminated by the addition of sample loading buffer. The mixtures were then subjected to the Mn^{2+}-Phos-tag SDS-PAGE (12% polyacrylamide gel including 50 μm $MnCl_2$ and Phos-tag acrylamide), and analyzed by western blotting using anti-XBP-1 antibody.

Cell death analysis

Post-treatment cell viability was determined by staining with propidium iodide (PI, 2 μg/ml) and flow cytometric analysis on a FACScan.

Patients and tissue specimens

In this study, the paraffin-embedded pathologic specimens from 229 patients with CRC were obtained from the archives of Department of Pathology, Cancer Center, Sun Yat-Sen University

and Guangdong Provincial People's Hospital, Guangzhou, China, between January 2000 and November 2006. The cases selected were based on distinctive pathologic diagnosis of CRC, undergoing primary and curative resection for CRC, availability of resection tissue and followup data, and had not received preoperative anticancer treatment. These CRC cases included 142 (62.0%) men and 87 (38.0%) women, with mean age of 57.3 years. Average followup time was 55.42 months (median, 60.0 months; range, 0.5-98 months). Patients whose cause of death remained unknown were excluded from our study. Clinicopathologic characteristics for these patients were summarized in Table 1. This study was approved by the medical ethics committee of our institutes.

Tissue microarray (TMA) and IHC

TMAs were constructed in accordance with a previously described method [49]. Triplicate 0.6 mm diameter cylinders were punched from representative areas of an individual donor tissue block, and re-embedded into a recipient paraffin block in a defined position, using a tissue arraying instrument (Beecher Instruments, Silver Spring, MD, USA).

The TMA blocks were cut into 5-μm sections and processed for IHC. TMA slides were incubated with anti-XBP-1 (1:100), anti-FoxO1 (1:50) and anti-p62 (1:200), respectively, and stored overnight at 4 °C. Immunostaining was performed using the Envision System with diaminobenzidine (Dako, Glostrup, Denmark). A negative control was obtained by replacing the primary antibody with a normal rabbit IgG. For the case of non-informative TMA samples (i.e., samples with < 500 tumor cells per case and lost samples), IHC staining was performed by using whole-tissue slides.

Positive expressions of XBP-1, FoxO1 and p62 in CRC tissues were primarily cytoplasmic patterns with a few cells showing nuclear staining (Figure 7C and 7D). Thus, in this study, we assessed the cytoplasmic expressions of the 3 proteins in our cohort of 229 CRC tissues. A semi-quantitative scoring criterion for IHC of XBP-1, FoxO1 and p62 was used, in which both staining intensity and positive areas were recorded. A staining index (values 0-12), obtained as the intensity of XBP-1, FoxO1 and p62 positive staining (negative = 0, weak = 1, moderate = 2 or strong = 3 scores) and the proportion of immunostaining positive cells of interest (< 25% = 1, 25%-50% = 2, > 50% – < 75% = 3, ≥ 75% = 4 scores) were calculated. The mean staining index of XBP-1, FoxO1 and p62 in this CRC cohort was 5.2, 2.7 and 6.3. Thus, categories of high expressions of XBP-1, FoxO1 and p62 were defined as CRC cases with staining index of more than 5.2, 2.7 and 6.3, respectively. Two independent pathologists (M-Y Cai and D Xie) blinded to the clinic pathologic information performed the scorings. The inter-observer disagreements were reviewed a second time, followed by a conclusive judgment by both pathologists.

Statistical analysis

Statistical analysis was performed by using the SPSS statistical software package (standard version 13.0; SPSS Inc., Chicago, IL, USA). The correlations between molecular features detected with each other and the associations between expressions of XBP-1, FoxO1 and p62, and CRC patients' clinic pathological features were assessed by the Chi-square test. For univariate survival analysis, survival curves were obtained with the Kaplan-Meier method. The Cox proportional hazards regression model was used to identify the independent prognostic factors. $P < 0.05$ were considered statistically significant.

Acknowledgments

This study was supported by the Ministry of Science and Technology of China (2011CB910100 to YZ; 2011CB504200 to WZ), Program for New Century Excellent Talents in University, the National Natural Science Foundation of China (81222028, 30900722, 31070691 and 30921062), and "111 project" from the Minister of Education of China.

References

1 Mizushima N. Autophagy: process and function. *Genes Dev* 2007; **21**:2861-2873.
2 Levine B, Klionsky DJ. Development by self-digestion: molecular mechanisms and biological functions of autophagy. *Dev Cell* 2004; **6**:463-477.
3 Klionsky DJ, Emr SD. Autophagy as a regulated pathway of cellular degradation. *Science* 2000; **290**:1717-1721.
4 Mizushima N, Komatsu M. Autophagy: renovation of cells and tissues. *Cell* 2011; **147**:728-741.
5 Kroemer G, Marino G, Levine B. Autophagy and the integrated stress response. *Mol Cell* 2010; **40**:280-293.
6 Massey AC, Follenzi A, Kiffin R, Zhang C, Cuervo AM. Early cellular changes after blockage of chaperone-mediated autophagy. *Autophagy* 2008; **4**:442-456.
7 Yu L, McPhee CK, Zheng L, *et al.* Termination of autophagy and reformation of lysosomes regulated by mTOR. *Nature* 2010; **465**:942-946.
8 Ravikumar B, Vacher C, Berger Z, *et al.* Inhibition of mTOR induces autophagy and reduces toxicity of polyglutamine expansions in fly and mouse models of Huntington disease. *Nat Genet* 2004; **36**:585-595.
9 Liang XH, Jackson S, Seaman M, *et al.* Induction of autophagy and inhibition of tumorigenesis by beclin 1. *Nature* 1999; **402**:672-676.
10 Zhao Y, Yang J, Liao W, *et al.* Cytosolic FoxO1 is essential for the induction of autophagy and tumour suppressor activity. *Nat Cell Biol* 2010; **12**:665-675.
11 Zhao J, Brault JJ, Schild A, *et al.* FoxO3 coordinately activates protein degradation by the autophagic/lysosomal and proteasomal pathways in atrophying muscle cells. *Cell Metab* 2007; **6**:472-483.
12 Mammucari C, Milan G, Romanello V, *et al.* FoxO3 controls autophagy in skeletal muscle *in vivo*. *Cell Metab* 2007; **6**:458-471.
13 Greer EL, Brunet A. FOXO transcription factors at the interface between longevity and tumor suppression. *Oncogene* 2005; **24**:7410-7425.
14 Kenyon C, Chang J, Gensch E, Rudner A, Tabtiang R. A *C. elegans* mutant that lives twice as long as wild type. *Nature* 1993; **366**:461-464.
15 Lee SS, Kennedy S, Tolonen AC, Ruvkun G. DAF-16 target genes that control *C. elegans* life-span and metabolism. *Science* 2003; **300**:644-647.
16 Lin K, Dorman JB, Rodan A, Kenyon C. daf-16: An HNF-3/

forkhead family member that can function to double the life-span of *Caenorhabditis elegans*. *Science* 1997; **278**:1319-1322.
17 Fu Z, Tindall DJ. FOXOs, cancer and regulation of apoptosis. *Oncogene* 2008; **27**:2312-2319.
18 Zhou J, Liao W, Yang J, *et al.* FOXO3 induces FOXO1-dependent autophagy by activating the AKT1 signaling pathway. *Autophagy* 2012; **8**:1712-1723.
19 Juhasz G, Puskás LG, Komonyi O, *et al.* Gene expression profiling identifies FKBP39 as an inhibitor of autophagy in larval *Drosophila* fat body. *Cell Death Differ* 2007; **14**:1181-1190.
20 Huang H, Regan KM, Wang F, *et al.* Skp2 inhibits FOXO1 in tumor suppression through ubiquitin-mediated degradation. *Proc Natl Acad Sci USA* 2005; **102**:1649-1654.
21 Kato S, Ding J, Pisck E, Jhala US, Du K. COP1 functions as a FoxO1 ubiquitin E3 ligase to regulate FoxO1-mediated gene expression. *J Biol Chem* 2008; **283**:35464-35473.
22 Yang JY, Zong CS, Xia W, *et al.* ERK promotes tumorigenesis by inhibiting FOXO3a via MDM2-mediated degradation. *Nat Cell Biol* 2008; **10**:138-148.
23 Fu W, Ma Q, Chen L, *et al.* MDM2 acts downstream of p53 as an E3 ligase to promote FOXO ubiquitination and degradation. *J Biol Chem* 2009; **284**:13987-14000.
24 Zhou Y, Lee J, Reno CM, *et al.* Regulation of glucose homeostasis through a XBP-1-FoxO1 interaction. *Nat Med* 2011; **17**:356-365.
25 Shajahan AN, Riggins RB, Clarke R. The role of X-box binding protein-1 in tumorigenicity. *Drug News Perspect* 2009; **22**:241-246.
26 Yamamoto K, Yoshida H, Kokame K, Kaufman RJ, Mori K. Differential contributions of ATF6 and XBP1 to the activation of endoplasmic reticulum stress-responsive *cis*-acting elements ERSE, UPRE and ERSE-II. *J Biochem* 2004; **136**:343-350.
27 Yoshida H, Matsui T, Yamamoto A, Okada T, Mori K. XBP1 mRNA is induced by ATF6 and spliced by IRE1 in response to ER stress to produce a highly active transcription factor. *Cell* 2001; **107**:881-891.
28 Yoshida H, Matsui T, Hosokawa N, Kaufman RJ, Nagata K, Mori K. A time-dependent phase shift in the mammalian unfolded protein response. *Dev Cell* 2003; **4:**265-271.
29 Vidal RL, Figueroa A, Court FA, *et al.* Targeting the UPR transcription factor XBP1 protects against Huntington's disease through the regulation of FoxO1 and autophagy. *Hum Mol Genet* 2012; **21**:2245-2262.
30 Hetz C, Thielen P, Matus S, *et al.* XBP-1 deficiency in the nervous system protects against amyotrophic lateral sclerosis by increasing autophagy. *Genes Dev* 2009; **23**:2294-2306.
31 Shvets E, Fass E, Elazar Z. Utilizing flow cytometry to monitor autophagy in living mammalian cells. *Autophagy* 2008; **4**:621-628.
32 Matsuzaki H, Daitoku H, Hatta M, Tanaka K, Fukamizu A. Insulin-induced phosphorylation of FKHR (Foxo1) targets to proteasomal degradation. *Proc Natl Acad Sci USA* 2003; **100**:11285-11290.
33 Aoki M, Jiang H, Vogt PK. Proteasomal degradation of the FoxO1 transcriptional regulator in cells transformed by the P3k and Akt oncoproteins. *Proc Natl Acad Sci USA* 2004; **101**:13613-13617.
34 Massey AC, Kaushik S, Sovak G, Kiffin R, Cuervo AM. Consequences of the selective blockage of chaperone-mediated autophagy. *Proc Natl Acad Sci USA* 2006; **103**:5805-5810.
35 Bejarano E, Cuervo AM. Chaperone-mediated autophagy. *Proc Am Thorac Soc* 2010; **7**:29-39.
36 Plas DR, Thompson CB. Akt activation promotes degradation of tuberin and FOXO3a via the proteasome. *J Biol Chem* 2003; **278**:12361-12366.
37 Yoshida H, Uemura A, Mori K. pXBP1(U), a negative regulator of the unfolded protein response activator pXBP1(S), targets ATF6 but not ATF4 in proteasome-mediated degradation. *Cell Struct Funct* 2009; **34**:1-10.
38 Yoshida H, Oku M, Suzuki M, Mori K. pXBP1(U) encoded in XBP1 pre-mRNA negatively regulates unfolded protein response activator pXBP1(S) in mammalian ER stress response. *J Cell Biol* 2006; **172**:565-575.
39 Lee J, Sun C, Zhou Y, *et al.* p38 MAPK-mediated regulation of Xbp1s is crucial for glucose homeostasis. *Nat Med* 2011; **17**:1251-1260.
40 Shintani T, Klionsky DJ. Autophagy in health and disease: a double-edged sword. *Science* 2004; **306**:990-995.
41 Baehrecke EH. Autophagy: dual roles in life and death? *Nat Rev Mol Cell Biol* 2005; **6**:505-510.
42 Levine B, Yuan J. Autophagy in cell death: an innocent convict? *J Clin Invest* 2005; **115**:2679-2688.
43 Edinger AL, Thompson CB. Death by design: apoptosis, necrosis and autophagy. *Curr Opin Cell Biol* 2004; **16**:663-669.
44 Moreau K, Luo S, Rubinsztein DC. Cytoprotective roles for autophagy. *Curr Opin Cell Biol* 2010; **22**:206-211.
45 Denton D, Nicolson S, Kumar S. Cell death by autophagy: facts and apparent artefacts. *Cell Death Differ* 2012; **19**:87-95.
46 Gozuacik D, Kimchi A. Autophagy as a cell death and tumor suppressor mechanism. *Oncogene* 2004; **23**:2891-2906.
47 Romero-Ramirez L, Cao H, Regalado MP, *et al*. X box-binding protein 1 regulates angiogenesis in human pancreatic adenocarcinomas. *Transl Oncol* 2009; **2**:31-38.
48 Koong AC, Chauhan V, Romero-Ramirez L. Targeting XBP-1 as a novel anti-cancer strategy. *Cancer Biol Ther* 2006; **5**:756-759.
49 Xie D, Ma NF, Pan ZZ, *et al.* Overexpression of EIF-5A2 is associated with metastasis of human colorectal carcinoma. *Hum Pathol* 2008; **39**:80-86.

(**Supplementary information** is linked to the online version of the paper on the *Cell Research* website.)